Modelling the role of local correlations in polycrystal plasticity using viscoplastic self-consistent schemes

R Lebensohn

IFIR (UNR-CONICET), 27 de Febrero 210 Bis, 2000 Rosario, Argentina

Abstract. A viscoplastic self-consistent (VPSC) multiscale model for predicting the plastic behaviour of materials with lamellar microstructures is presented. In this approach, three different scales are defined: the microscopic, at single crystal (single lamella) scale; the mesoscopic, at the scale of a single lamellar colony and the macroscopic, at the lamellar aggregate level. This formulation is compared with the two-site VPSC model and both are applied to the prediction of the plastic anisotropy of an as-cast sample of a lamellar γ-TiAl based alloy (Ti–48 at%Al–2 at%Cr) tested under compression.

1. Introduction

The viscoplastic self-consistent (VPSC) theory for the prediction of the large strain behaviour of heterogeneous materials has been extensively used in the theory of plastic anisotropy and texture development of polycrystals. The general n-site VPSC theory was originally formulated by Molinari–Canova–Ahzi [1]. In their precursor paper they implemented the calculation of texture development of a face-centred-cubic (fcc) material using a one-site approximation and assuming isotropic behaviour of the homogeneous equivalent medium (HEM). Later, Lebensohn and Tomé [2] implemented a fully anisotropic one-site VPSC code which has been applied by several authors to a wide variety of materials [2–11]. Nevertheless, the applications of this one-site VPSC formulation are limited essentially to single phase polycrystals. This is due to the fact that under this approach the polycrystal is regarded as a perfectly disordered aggregate of single crystals which undergo local homogeneous deformation. This scenario does not represent a number of materials in which the local interaction between crystals of different phases and/or the local crystallographic, morphologic and topologic correlations between neighbour crystallites do exist and have a non-negligible influence on the overall behaviour of the aggregate.

The first attempt to extend the applications of the VPSC theory to deal with multiphase, locally correlated polycrystals is due to Canova *et al* [12] who developed a first-neighbour n-site program. This code has been applied only once, i.e. for the prediction of texture development of a two-phase quartz-mica aggregate [12] and it is currently being revisited by Solas and Tomé [13]. On the other hand, Lebensohn and Canova [14] developed a two-site (VPSC-2S) approach that considers the interaction of two inclusions (usually representing neighbour crystallites of different phases) embedded in a HEM. This two-site approach has been successfully applied to explain the differences in the texture development of $(\alpha + \beta)$ Ti alloys of different microstructures. Particularly in the case of a lamellar $(\alpha + \beta)$ Ti alloy (for which each pair of inclusions represents a complete stack of lamellae or *lamellar colony*)

the VPSC-2S simulations help us to understand the link between the local correlations given by the Burgers relationship between the α- and β-phases and the rolling textures developed in the material [14].

Following our efforts to extend the VPSC model to new applications, we present in this paper a multiscale approach (still in the frame of a one-site VPSC formulation) to predict the plastic anisotropy of an aggregate of lamellar colonies. In this case, instead of the classical two micro- and macroscales at single crystal and polycrystal levels, respectively, three different scales are defined: the microscopic scale, at single crystal (i.e. a single lamella) level; the mesoscopic scale, at the lamellar colony level and the macroscopic scale, at the lamellar aggregate level. The constitutive behaviour at the mesoscopic level is based on [15]: (a) the assumption of an overall state in each colony, given by a weighted average in the lamellae; (b) the rate-sensitivity equation to describe crystal plasticity by slip and twinning inside each lamella; (c) the relaxed constraints (RC) theory [16] to allow variations of some stress and strain rate components, according to the morphology of the lamellae; and (d) the assignment of critical stresses to the slip and twinning systems according to a classification based on the relative orientation of those with respect to the habit plane of the lamellar structure.

The aim of this paper is first to present the main equations of this VPSC model for lamellar structures (VPSC-LS) and then use and compare the ability of the VPSC-LS and the VPSC-2S models to reproduce the strong plastic anisotropy observed in a lamellar γ-TiAl based alloy [17]. This strong plastic anisotropy has been measured in an as-cast sample of composition Ti–48 at%Al–2 at%Cr. The habit plane of the lamellar colonies (or *polysynthetically twinned (PST) crystals*) are strongly oriented along one direction of the sample. This material was tested in compression at different angles with respect to the main orientation of the lamellae.

2. Models

The rate-sensitivity equation relating the stress and strain rate at single crystal level is given by

$$\dot{\varepsilon} = \dot{\gamma}_0 \sum_s m^s \left(\frac{m^s : \sigma'}{\tau_0^s} \right)^n \tag{1}$$

where τ_0^s and m^s are the critical stress and the Schmid tensor of system (s); $\dot{\gamma}_0$ is a reference strain-rate and n is the inverse of the rate sensitivity. The initial values of τ_0^s are usually assumed to be equal for each system of the same deformation mode. Particularly, in a face-centred tetragonal (fct) γ-TiAl single crystal the active deformation systems are [18]: four systems of the $\{111\}\langle110]$ ordinary slip mode, eight systems of the $\{111\}\langle101]$ super slip mode and four systems of the $\{111\}\langle11\bar{2}]$ twinning mode. However, if a γ-TiAl crystallite is part of a lamellar structure it can be rationally assumed that the morphology determines differences between the critical stresses of deformation systems of the same mode, at very early stages of deformation, i.e. the critical stress may be different for systems of the same slip or twinning mode depending on the orientation of each system with respect to the lamellar plane. These considerations lead to a new *morphology-based* classification of the deformation systems [15]. In this sense, it is possible to find in each lamella one ordinary slip system, two super slip systems and one twinning system which have their slip (or twinning) direction and slip (or twinning) plane parallel to the interface. These slip (or twinning) systems are grouped in the *longitudinal slip (or twinning) mode*. Each lamella also contains one ordinary slip system and two super slip systems with their slip direction parallel to the interface and with the slip plane transversal to the interface. These slip systems correspond to the *mixed slip mode*. Finally, the rest of the ordinary, super and twinning systems have their slip (or twinning) directions and their slip

(or twinning) planes transversal to the interface. These slip (or twinning) systems belong to *transversal slip (or twinning) mode*.

At this point it is useful to remind ourselves of some basic equations of the one-site VPSC formulation. Using the notation of Lebensohn and Tomé [2] the micro–macro connection in the model is given by the *interaction equation*

$$\dot{E} + \tilde{M}:\Sigma' - (\dot{\varepsilon} + \tilde{M}:\sigma') = 0 \tag{2}$$

where $(\dot{E}, \Sigma')$ is the macroscopic strain-stress rate stress state and $\tilde{M}$ is the interaction tensor, a function of the viscoplastic Eshelby tensor S and the macroscopic tangent compliance M^{tg}

$$\tilde{M} = (I - S)^{-1}:S:M^{\text{tg}}. \tag{3}$$

Once M^{tg} is adjusted self-consistently (see [2] for details) and using (1) and (3) in (2), the local state for each single crystal in the aggregate can be obtained by solving a 5×5 system of nonlinear equations. The macroscopic state can then be calculated as a weighted average of the local states solution.

2.1. The two-site VPSC model

The VPSC-2S model can be used to simulate the plastic behaviour of a γ-TiAl based alloy. As in the case of a lamellar $(\alpha + \beta)$ Ti alloy, each pair of inclusions should represent a lamellar colony. For this purpose, some simplifications are required. On the one hand, the lamellar colony should be assumed to be represented by two fct lamellae [15] instead of the so-called *six-domain structure* [19] and, on the other hand, any influence of the minority α_2-Ti$_3$Al phase [19] should be neglected.

The crystallographic orientations of both interacting sites should be related through the twinning relationship. From a morphological point of view both sites should be flat ellipsoids. These ellipsoids should be tangent and aligned along the direction of their common short axis, which should be normal to the twinning plane.

The complete VPSC-2S theory can be found elsewhere [14] and will not be repeated in this work but we present here the interaction equation for the two-site case. If the two sites are identified as M (matrix) and T (twin), the interaction equation can be written as

$$\dot{E} + (\tilde{M}^{MM} + \tilde{M}^{MT}):\Sigma' - (\dot{\varepsilon}^M + \tilde{M}^{MM}:\sigma'^M + \tilde{M}^{MT}:\sigma'^T) = 0$$
$$\dot{E} + (\tilde{M}^{TM} + \tilde{M}^{TT}):\Sigma' - (\dot{\varepsilon}^T + \tilde{M}^{TM}:\sigma'^M + \tilde{M}^{TT}:\sigma'^T) = 0 \tag{4}$$

where $(\dot{\varepsilon}^M, \sigma'^M)$ and $(\dot{\varepsilon}^T, \sigma'^T)$ are the local states inside the matrix and the twin, $\tilde{M}^{MM}$ and $\tilde{M}^{TT}$ are the ordinary one-site interaction tensors defined in (3) and $\tilde{M}^{MT}$ and $\tilde{M}^{TM}$ are the two-site interaction tensors which are a function of the shape and relative volume and orientation of both sites and the tangent compliance of the HEM (explicit expressions are given in [14]). Using equation (1) in (4) the local states in both sites can be obtained by solving a 10×10 system of nonlinear equations.

2.2. The VPSC model for lamellar structures

Let us continue by considering the simplified γ-TiAl lamellar structure formed by one matrix and one twin. If the matrix-twin pair corresponds to a $(\bar{1}\bar{1}1)[\bar{1}\bar{1}\bar{2}]$ twinning system it is convenient to adopt a reference frame having axis x_3^L lying along the twinning direction $[\bar{1}\bar{1}\bar{2}]$, axis x_2^L along $[\bar{1}\bar{1}1]$ (i.e. normal to the twinning plane) and axis x_1^L along $[1\bar{1}0]$. Based on the RC theory, when a strain rate $\bar{\dot{\varepsilon}}_i$ is applied to the matrix–twin structure the constitutive relation

of the lamellar structure in that particular reference frame can be written as [15]

$$\bar{\dot{\varepsilon}}_i - \dot{\gamma}_0\left(w^M\sum_s m_i^{s,M}\left(\frac{m_j^{s,M}\sigma_j'^M}{\tau_0^{s,M}}\right)^n + w^t\sum_s m_i^{s,T}\left(\frac{m_j^{s,T}\sigma_j'^T}{\tau_0^{s,T}}\right)^n\right) = 0 \tag{5a}$$

$$\dot{\varepsilon}_1^M = \dot{\varepsilon}_1^T \tag{5b}$$

$$\dot{\varepsilon}_2^M = \dot{\varepsilon}_2^T \tag{5c}$$

$$\dot{\varepsilon}_3^M = \dot{\varepsilon}_3^T \tag{5d}$$

$$\sigma_4'^M = \sigma_4'^T \tag{5e}$$

$$\sigma_5'^M = \sigma_5'^T \tag{5f}$$

where s, M and s, T identify the slip and twinning systems in both lamellae; w^M and w^T are weight factors proportional to the relative volumes of matrix and twin, respectively. In (5), the traceless tensors are expressed as five-dim vectors using a modified [15] (third and fourth components are interchanged) Lequeu convention [20]. The overall stress in the lamellar structure can be obtained as

$$\bar{\sigma}_j' = w^M\sigma_j'^M + w^T\sigma_j'^T. \tag{6}$$

Regarding each single lamellar structure in a polycrystal as an inclusion embedded in an equivalent medium, it is possible to write an interaction equation, expressed by the following 10×10 system of nonlinear equations

$$\dot{E}_i + \tilde{M}_{ij}\sigma_j' - \dot{\gamma}_0\left(w^M\sum_s m_i^{s,M}\left(\frac{m_j^{s,M}\sigma_j'^M}{\tau_0^{s,M}}\right)^n + w^t\sum_s m_i^{s,T}\left(\frac{m_j^{s,T}\sigma_j'^T}{\tau_0^{s,T}}\right)^n\right)$$
$$- \tilde{M}_{ij}(w^M\sigma'^M + w^T\sigma'^T) = 0 \tag{7a}$$

$$\dot{\varepsilon}_1^M = \dot{\varepsilon}_1^T \tag{7b}$$

$$\dot{\varepsilon}_2^M = \dot{\varepsilon}_2^T \tag{7c}$$

$$\dot{\varepsilon}_3^M = \dot{\varepsilon}_3^T \tag{7d}$$

$$\sigma_4'^M = \sigma_4'^T \tag{7e}$$

$$\sigma_5'^M = \sigma_5'^T \tag{7f}$$

where $\tilde{M}$ is given by equation (3). The self-consistent equation for the iterative adjustment of the macroscopic tangent compliance M^{tg} is given by [2]

$$M^{\text{tg}} = \bar{M}^{\text{tg}}:\left(\frac{1}{n}\bar{M}^{\text{tg}} + \tilde{M}\right)^{-1}:\left(\frac{1}{n}M^{\text{tg}} + \tilde{M}\right). \tag{8}$$

Consequently, the calculation of the tangent compliance of the lamellar structure

$$\bar{M}^{\text{tg}} = \frac{\mathrm{d}\bar{\varepsilon}}{\mathrm{d}\bar{\sigma}'} \tag{9}$$

is an essential part of this formulation. The following derivation of $\bar{M}^{\text{tg}}$ is due to Canova and Lebensohn [21]. The RC conditions can be written as follows

$$K:(\dot{\varepsilon}^M - \bar{\dot{\varepsilon}}) = \bar{\sigma}' - \sigma'^M \qquad\qquad K:(\dot{\varepsilon}^T - \bar{\dot{\varepsilon}}) = \bar{\sigma}' - \sigma'^T \tag{10}$$

where K is an auxiliary matrix given by

$$K = \begin{bmatrix} \infty & 0 & 0 & 0 & 0 \\ 0 & \infty & 0 & 0 & 0 \\ 0 & 0 & \infty & 0 & 0 \\ 0 & 0 & 0 & 0 & 0 \\ 0 & 0 & 0 & 0 & 0 \end{bmatrix}. \tag{11}$$

Then

$$d\sigma'^M = [K:M^{\text{tg},M} + I]^{-1}:[K:M^{\text{tg},T} + I]:d\sigma'^T = A:d\sigma'^T. \tag{12}$$

From (12) it is possible to derive

$$d\bar{\varepsilon} = [w^M M^{\text{tg},M}:A + w^T M^{\text{tg},T}]:d\sigma'^T \tag{13}$$

$$d\sigma'^T = [w^M A + w^T I]^{-1}:d\bar{\sigma}' \tag{14}$$

and finally

$$\bar{M}^{\text{tg}} = [w^M M^{\text{tg},M}:A + w^T M^{\text{tg},T}]:[w^M A + w^T I]^{-1}. \tag{15}$$

3. Results

Figure 1 shows the crystallographic and morphologic texture of an as-cast sample of composition Ti–48 at%Al–2 at%Cr. The lamellae are strongly oriented along the x_2 direction of the sample. This material was tested under uniaxial compression at different angles in the x_2–x_3 plane. The angle ϕ is the tilt angle of the compression axis, measured from x_3 in that plane. For each test, the yield stresses and the relative transversal strains were measured [17].
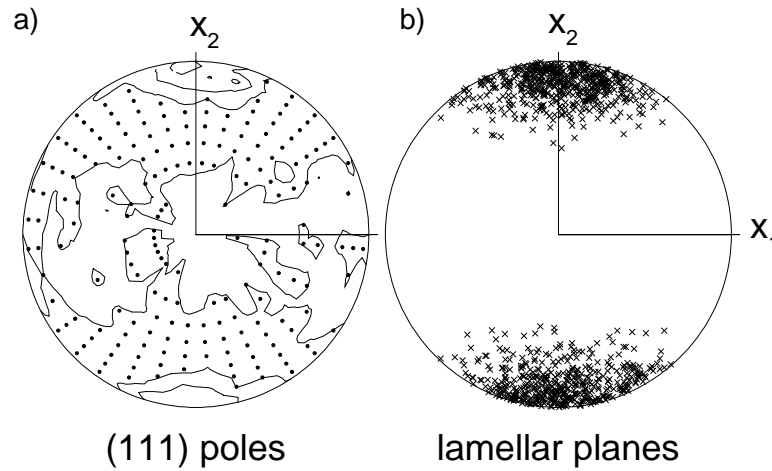
Figure 1. (a) Crystallographic and (b) morphologic textures of the as-cast sample of composition Ti–48 at%Al–2 at%Cr.

Both the VPSC-LS and the VPSC-2S models were used to reproduce the measured stress and strain anisotropy of the as-cast sample. The input texture was obtained from the measured orientation distribution function (ODF) [17]. The inverse of the rate-sensitivity is taken as $n = 19$. Other relevant input parameters are the critical stresses of the longitudinal, mixed and transversal modes. In this work we tested two different combinations corresponding to a lower and a higher anisotropy induced by the lamellae morphology. The combination of higher anisotropy is the one obtained by a fitting procedure performed on a single γ-TiAl PST crystal [15], i.e. $\tau_0^{\text{long}} = 1.0$, $\tau_0^{\text{mix}} = 2.72$ and $\tau_0^{\text{trans}} = 3.33$ (arbitrary units). On the other hand, the combination of lower anisotropy is: $\tau_0^{\text{long}} = 1.0$, $\tau_0^{\text{mix}} = 1.75$ and $\tau_0^{\text{trans}} = 2.0$. The PST inclusions were assumed to be cigar-shaped ellipsoids elongated in the x_2 direction (i.e. a shape which resembles the actual morphology of the colonies).

The (a) measured and predicted yield stresses (relative to the yield stress at $\phi = 90$), the (b) relative transversal strains and the calculated activity of the different deformation modes
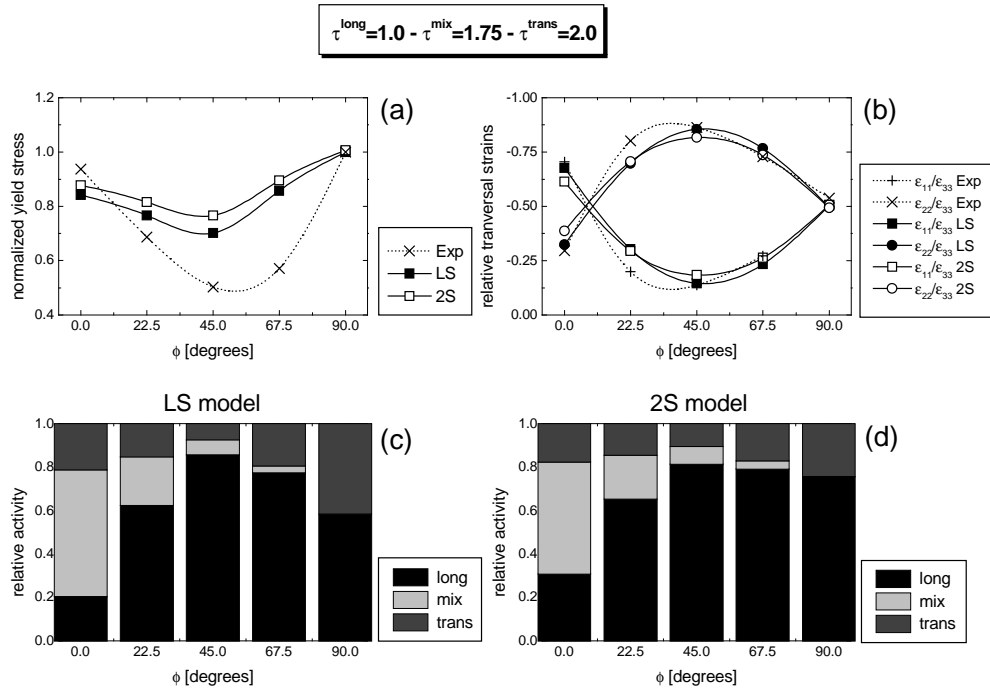
Figure 2. (a) Relative anisotropy of yield stresses: measurements on the Ti–48 at%Al–2 at%Cr as-cast sample [17] and model predictions assuming: $\tau_0^{\text{long}} = 1.0$, $\tau_0^{\text{mix}} = 1.75$ and $\tau_0^{\text{trans}} = 2.0$. (b) Same as (a) for relative transversal strains. (c) Relative activities of the deformation modes, predicted with the VPSC-LS model. (d) Same as (c) for the VPSC-2S model.

obtained with the (c) VPSC-LS and the (d) VPSC-2S models for the cases of lower and higher anisotropy are shown in figures 2 and 3, respectively. In general, the model predictions show a good qualitative agreement with the experiments. The observed yield stress dependence with angle ϕ and the drastic changes of the relative transversal strain are well reproduced by both models and for both combinations of critical stresses.

Plots of the relative activities show the role that each deformation mode plays at different angles. The hard mixed and transversal slip are particularly active at $0°$ and $90°$, respectively and the more angle ϕ deviates from $0°$ and $90°$, the less active those hard modes become. The soft longitudinal slip and twinning modes—which accommodate a significant part of the strain, for every orientation of the compression axis—are most active at $45°$. A similar dependence of the mode of active deformation mechanism was obtained with the single PST model [15] but with extremely sharp changes of the predicted activities: 100% of mixed slip, transversal slip and longitudinal slip and twinning were obtained for $0°$, $90°$ and intermediate angles, respectively. In the present case, the texture softens that sharp behaviour and, due to the local deviations of the lamellar plane orientation, different deformation modes are favoured in different grains for the same macroscopic orientation of the sample.

In the lower anisotropy case (figure 2) the results obtained with both models for stresses, strains and relative activity are very similar but in particular the stress anisotropy is underestimated. In the higher anisotropy case (figure 3), using the values of critical stresses fitted to reproduce the anisotropy of PST crystals, a better matching between the measured stress anisotropy and the predictions of the VPSC-LS model is observed. The VPSC-2S predictions show the same trend but the differences between the yield stresses at $0°$ and $90°$

$$\tau^{long}=1.0 - \tau^{mix}=2.72 - \tau^{trans}=3.33$$
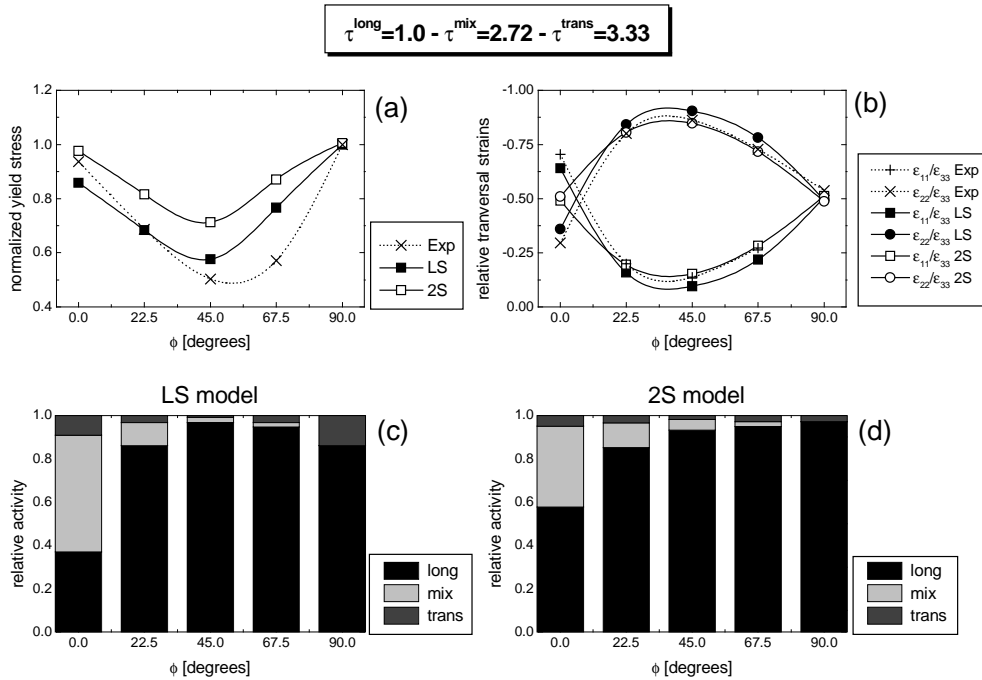
Figure 3. (a) Relative anisotropy of yield stresses: measurements on the Ti–48 at%Al–2 at%Cr as-cast sample [17] and model predictions assuming: $\tau_0^{long} = 1.0$, $\tau_0^{mix} = 2.72$ and $\tau_0^{trans} = 3.33$. (b) Same as (a), for relative transversal strains. (c) Relative activities of the deformation modes, predicted with the VPSC-LS model. (d) Same as (c), for the VPSC-2S model.

and at intermediate angles are not as pronounced as in the experiments. The most important disagreement between the experiments and the VPSC-LS predictions on the one hand and the VPSC-2S predictions on the other hand correspond to the relative transversal strains at $0°$. While the VPSC-LS reproduces the measured values which deviate significantly from axial symmetry, the VPSC-2S predicts an axisymmetric behaviour. The reason for this discrepancy between both models can be explained in terms of the differences between the predicted activities in the $0°$ case. Comparing figures 3(c) and 3(d) it is evident that the activity of the mixed slip mode is significantly lower in the 2S than in the LS case. Furthermore, in the 2S case most of the strain is still accommodated by the soft longitudinal systems, even if they are not well oriented relative to the compression direction. This means that, compared with the LS model, the 2S results exhibit a higher trend to enforce stress equilibrium in detriment to strain compatibility.

4. Conclusions

(1) The VPSC-2S and the VPSC-LS models were used to predict the plastic anisotropy of a textured γ-TiAl based alloy with lamellar structure. Both models give a generally good qualitative agreement with the observed anisotropy. This result validates the use of the VPSC-LS, which is still a (modified) one-site approach, as an alternative to the more complex two-site formulation to account for the influence of the local correlations on the plastic behaviour of polycrystals.

(2) For the alloy studied in this work the combination of critical stresses that fit the plastic anisotropy of a single PST crystal, when used in the VPSC-LS, also gives good predictions of the anisotropy of a textured lamellar polycrystal.

References

[1] Molinari A, Canova G R and Ahzi S 1987 A selfconsistent approach of the large deformation polycrystal viscoplasticity *Acta Metall.* **35** 2983–94
[2] Lebensohn R and Tomé C N 1993 A self-consistent approach for the simulation of plastic deformation and texture development of polycrystals: application to zirconium alloys *Acta Metall. Mater.* **41** 2611–24
[3] Lebensohn R, Sanchez P and Pochettino A 1994 Modelling texture development of zirconium alloys at high temperature *Scripta Metall. Mater.* **30** 481–6
[4] Lebensohn R and Tomé C N 1994 A self-consistent visco-plastic model: calculation of rolling textures of anisotropic materials *Mater. Sci. Eng.* A **175** 71–82
[5] Lebensohn R, Gonzalez M I, Pochettino A and Tomé C N 1996 Measurement and prediction of texture development during a rolling sequence of Zircaloy-4 tubes *J. Nucl. Mater.* **229** 57–64
[6] Castelnau O, Duval P, Lebensohn R and Canova G R 1996 Viscoplastic modelling of texture development in polycrystalline ice with a self-consistent approach: comparison with bound estimates *J. Geophys. Res.* B **101** 13 851–68
[7] Dunst D and Mecking H 1996 Analysis of experimental and theoretical rolling textures of two-phase titanium alloys *Z. Metallkd.* **87** 498–507
[8] Castelnau O, Canova G R, Lebensohn R and Duval P 1997 Modelling viscoplastic behavior of anisotropic polycrystalline ice with a selfconsistent approach *Acta Mater.* **45** 4828–34
[9] Maurice C and Driver J H 1997 Hot rolling textures of fcc metals—Part II. Numerical simulations *Acta Mater.* **45** 4639–49
[10] Lebensohn R, Wenk H R and Tomé C N 1998 Modelling deformation and recrystallization textures in calcite *Acta Mater.* **46** 2683–93
[11] Francillette H, Bacroix B, Gasperini M and Bechade J L 1998 Grain orientation effects in Zr702 polycrystalline samples deformed in channel die compression at room temperature *Acta Mater.* **46** 4131–42
[12] Canova G R, Wenk H R and Molinari A 1992 Deformation modelling of multiphase polycrystals: case of a quartz–mica aggregate *Acta Metall. Mater.* **40** 1519–30
[13] Solas D and Tomé C N 1998 Private communication
[14] Lebensohn R and Canova G R 1997 A selfconsistent approach for modelling texture development of two-phase polycrystals: application to titanium alloys *Acta Mater.* **45** 3687–94
[15] Lebensohn R, Uhlenhut H, Hartig C and Mecking H 1998 Plastic flow of γ-TiAl-based polysynthetically twinned crystals: micromechanical modelling and experimental validation *Acta Mater.* **46** 4701–9
[16] Honneff H and Mecking H 1981 Analysis of the deformation texture at different rolling conditions *Proc. ICOTOM-6* ed S Nagashima (Tokyo: The Iron and Steel Institute of Japan) pp 347–57
[17] Uhlenhut H 1998 Private communication
[18] Mecking H, Hartig C and Kocks U F 1996 Deformation modes in γ-TiAl as derived from the single crystal yield surface *Acta Mater.* **44** 1309–21
[19] Yamaguchi M 1991 Deformation and recrystallization behavior of the Ti–Al phase constituting the TiAl/Ti$_3$Al lamellar structure of Ti-rich TiAl compounds *ISIJ Int.* **31** 1127–33
[20] Lequeu P, Gilormini P, Montheillet F, Bacroix B and Jonas J J 1987 Yield surfaces for textured polycrystals—I. Crystallographic approach *Acta Metall.* **35** 439–51
[21] Canova G R and Lebensohn R 1996 unpublished work